Charge Ordering and Spin Dynamics in NaV_2O_5

B. Grenier,[1] O. Cepas,[2] L. P. Regnault,[1] J. E. Lorenzo,[3] T. Ziman,[2] J. P. Boucher,[4] A. Hiess,[2] T. Chatterji,[2] J. Jegoudez,[5] and A. Revcolevschi[5]

[1]*Département de Recherche Fondamentale sur la Matière Condensée, SPSMS, Laboratoire de Magnétisme et de Diffraction Neutronique, CEA-Grenoble, F-38054 Grenoble cedex 9, France*

[2]*Institut Laue Langevin, BP 156, F-38042 Grenoble cedex 9, France*

[3]*Laboratoire de Cristallographie, CNRS, BP 166, F-38042 Grenoble cedex 9, France*

[4]*Laboratoire de Spectrométrie Physique, Université J. Fourier Grenoble I, BP 87, F-38402 Saint Martin d'Hères cedex, France*

[5]*Laboratoire de Physico-Chimie de l'Etat Solide, Université Paris-Sud, Bât 414, F-91405 Orsay cedex, France*

(Received 23 June 2000)

We report high-resolution neutron inelastic scattering experiments on the spin excitations of NaV_2O_5. Below T_c, two branches with distinct energy gaps are identified. From the dispersion and intensity of the spin excitation modes, we deduce the precise zigzag charge distribution on the ladder rungs and the corresponding charge order: $\Delta_c \approx 0.6$. We argue that the spin gaps observed in the low-T phase of this compound are primarily due to the charge transfer.

DOI: 10.1103/PhysRevLett.86.5966 PACS numbers: 71.45.Lr, 75.10.Jm, 75.40.Gb

The low dimensional inorganic compound NaV_2O_5 undergoes a phase transition at $T_c = 34$ K [1] associated with both a lattice distortion [2] and the opening of an energy gap to the lowest triplet spin excitations [3]. While the nature of the low-T phase in NaV_2O_5 is not fully understood it is clear that, unlike CuGeO3, the spin-Peierls model does not apply simply to this compound [4]. The spin gap may result from charge order (CO) rather than the lattice distortion [5]. Indeed, NMR measurements indicate two inequivalent vanadium sites below T_c, while there exists only one site above [6]. There has been no direct evidence for the connection between CO and a spin gap, nor to distinguish various conjectured spatial distributions of charge [5,7]. In this Letter, we present new results of neutron inelastic scattering (NIS) on the spin excitations in the low-T phase that can now resolve these issues.

In NaV_2O_5, the vanadium ions have a formal valence of 4.5+. Initially, this was proposed to correspond to an alternation of V^{4+} ions, with a spin value $S = 1/2$, and V^{5+} ions with $S = 0$ [8]. At room temperature, NaV_2O_5 is well described by a quarter-filled two-leg ladder system, with only one type of vanadium site $V^{4.5+}$. From calculations of electronic structure [9,10], the strongest orbital overlaps are on the ladder rungs. One expects that the $S = 1/2$ spins are carried by the V-O-V molecular bonding orbitals, with charge fully delocalized on two sites. As the energy of the antibonding orbital is much higher, it can be projected out, and above T_c, these spins, as they interact in the leg direction ($\| \mathbf{b}$ axis), form an effective uniform quantum Heisenberg spin *chain* with interactions between chains that are both weaker and frustrated.

At low temperatures, NMR shows this can no longer be so. On each rung, a charge transfer Δ_c may occur. Taking the average charge on vanadium sites to be $1/2$, the charges on the two vanadium sites on a rung are defined through $n_\pm = (1 \pm \Delta_c)/2$. Two forms of CO can be considered [5], the *in line,* with the same charge transfer on each rung, and the *zigzag* with alternation in the charge along the ladders as shown in Fig. 1b. Recent x-ray diffraction measurements [11] established that the lattice structure below T_c consists of a succession of distorted and nondistorted ladders of vanadium ions (see Fig. 1a). Neglecting interladder diagonal couplings $J_\perp$, the ladders would behave magnetically as independent spin chains. For one ladder (chain 2 in Fig. 1a) distortions in the exchange paths both within the ladder and via neighboring ladders result in an alternation of the effective exchange coupling in the b directions, J_{b1} and J_{b2}. The ladders in which the rungs are distorted (chains 1 and 3), however, remain magnetically uniform as a mirror plane passes through each rung. A *minimum* magnetic model without CO would be a succession of alternating and uniform chains. An energy gap (expected to be small as it results primarily from the alternation in $J_\perp$) would characterize the excitation branch of

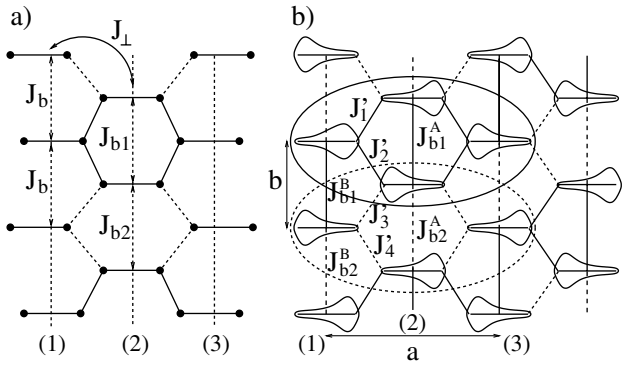

FIG. 1. (a) Simplified representation of distorted and nondistorted chains, chain 1 (or 3) and 2, respectively, with the $J_\perp$ bond alternation between chains 1 and 2; (b) proposed charge order (large and small lobes represent large and small average charges) leading to a spin gap. The elementary translation $(\mathbf{a}, \mathbf{b})$ of this CO agrees with the observed periodicity of spin excitations.

 0031-9007/01/86(26)/5966(4)$15.00

the alternating chains, and there would be no gap for the uniform chains. The initial NIS [3] found, however, two excitation branches, with the same gap at the antiferromagnetic (AF) point $E_g^+ = E_g^- \approx 10$ meV. To analyze these results, a recent spin model [12] used an explicit relation between the spin excitations and the CO. This model assumed a single gap and, as it implies zero intensity of one excitation branch, must be extended to explain the NIS data. A more precise determination of excitations in the low-T phase of NaV_2O_5 is therefore crucial. In the present work, using high resolution, the dispersion of the excitations is reexplored in a wider part of the reciprocal space. Moreover, the evaluation of the structure factor, i.e., the (energy-integrated) intensity of each excitation mode, allows us to determine the charge transfer Δ_c.

The single crystal ($\approx 8 \times 5 \times 2$ mm^3) was grown by a flux method. The NIS measurements were performed at $T \leq 4.2$ K, on two thermal neutron three-axes spectrometers — IN8 and CRG/CEA-IN22 — at the Institut Laue-Langevin (ILL). On IN8, vertically focusing monochromator PG(002) and Cu(111) were used in conjunction with a vertically focusing analyzer PG(002) and horizontal collimations 60′-40′-60′. The final wave vector was kept fixed at $k_f = 4.1$ Å^{-1}. IN22 was operated at $k_f = 2.662$ Å^{-1}, with a PG(002) monochromator and a PG(002) analyzer used in a horizontal monochromatic focusing condition [resulting wave-vector resolution: $\delta q \approx 0.03$ r.l.u. (reciprocal lattice units)] with no collimation. The sample was installed in an "orange" ILL cryostat, with the scattering wave vector **Q** lying in the reciprocal (a^*, b^*) ladder plane.

The two branches characterizing the low-energy excitations in NaV_2O_5 have distinct energy gaps: $E_g^+ \neq E_g^-$. This important result will be established when we consider the dispersions in the transverse **a** direction. First, however, we determine the dispersion in the leg direction (**b** axis). Examples of constant-energy scans obtained on IN8 as a function of Q_b are displayed in Fig. 2a (wave-vector components are expressed in r.l.u.). Increasing the energy, one resolves the single peak seen at 10 meV into propagating modes (dashed lines), whose peak position is shown in Fig. 2b. They describe the dispersion of the elementary excitations in the **b** direction, near the AF chain wave-vector component $Q_b^{\mathrm{AF}} (\equiv Q_b = 0.5)$. They are compared to a dispersion law characteristic of a gapped spin chain: $E(q_b) = \sqrt{E_g^2 + (E_m^2 - E_g^2)\sin^2(2\pi Q_b)}$, where E_g and E_m are the gap and maximum energies of the dispersion, respectively. For both $E_g = E_g^+, E_g^-$ (the solid and dashed lines, respectively), we evaluate $E_m = 93 \pm 6$ meV. Compared to the prediction for a uniform Heisenberg chain, $E_m = \pi J_b/2$, where J_b is the exchange in the chain, one obtains for the low-T phase, $J_b \approx 60$ meV.

Second, we consider the dispersions in the $\mathbf{a}^*$ direction (i.e., along the rungs). A few examples of energy scans performed on IN22 at constant **Q** are reported in Fig. 3. In general, two peaks are observed. At a few Q_a values, however, an extinction occurs. This extinction may

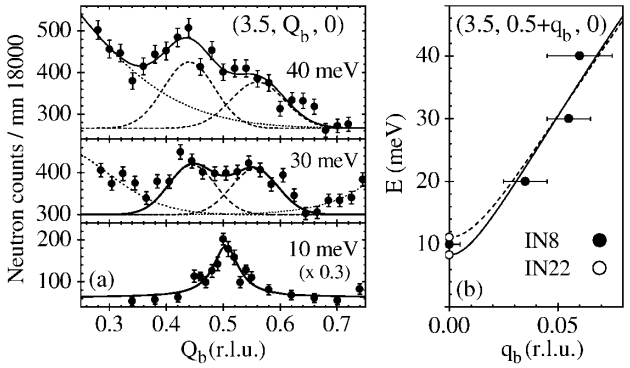

FIG. 2. IN8 data: (a) Constant-energy scans as a function of Q_b. The full lines are the results of fits to the data, which take into account both the magnetic contributions (shown as the dashed lines) and the background (the dotted line); (b) energy dispersion in the **b** direction. The lines correspond to the two branches with gaps E_g^+ and E_g^-.

concern one of the two modes, or the two modes simultaneously. The left and right panels report data obtained for $Q_b^{\mathrm{AF}} = 0.5$ and $Q_b = 1$ (equivalent to the zone center of the AF chains Q_b^{ZC}). As examples, we show for Q_b^{AF} that the smallest energy difference between the two observed peaks is obtained for *integer* Q_a values (here, $Q_a = 3$), the largest one for *half-integer* values ($Q_a = 2.5$), and an extinction of the two modes occurs at $Q_a \approx 1.75$ (identical results have been obtained for $Q_b = 1.5$). Surprisingly, at the chain zone center Q_b^{ZC} we found a small but nonzero intensity for the two excitation branches. The smallest energy difference between the two peaks is now obtained for half-integer values (here, $Q_a = 1.5$). Extinction of one of the two modes is observed at $Q_a = 1$ (on the high-energy mode) and at $Q_a = 2$ (on the low-energy mode). For all the spectra recorded on IN22, the background (the dotted lines in Fig. 3) was carefully determined. Several procedures have been used involving data recorded at low and high temperatures (i.e., above T_c). In Fig. 3a, for instance, the open dots used to define the background are obtained from measurements performed at 40 K [13] while

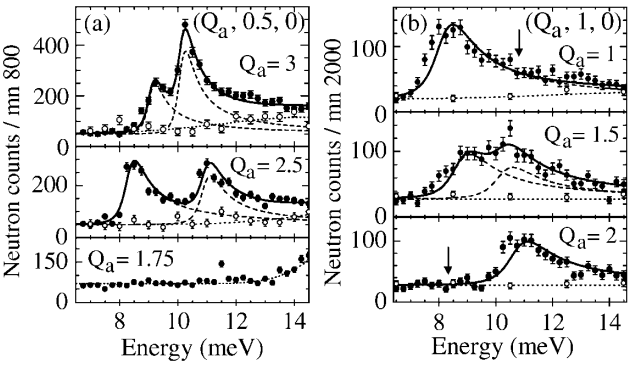

FIG. 3. IN12 data: Constant-**Q** scans as functions of energy. (a) At $Q_b \equiv Q_b^{\mathrm{AF}}$; (b) at $Q_b \equiv Q_b^{\mathrm{ZC}}$. The two arrows point to the positions expected for the two missing peaks. Curves are described in text.

in Fig. 1b, it is determined from Q_b scans performed at low temperature for different energies.

For the analysis, we assume the two observed peaks to belong to two distinct contributions. Their unsymmetrical line shape is characteristic of gapped excitations undergoing a rapid energy dispersion (as established in Fig. 2b). In such a case, a dynamical response function (shown by the dashed lines in Fig. 3) is well suited to fitting, conveniently defined with only three parameters: the peak energy $E_+(E_-)$, an intensity factor $A_+(A_-)$, and an energy damping Γ [14]. As Γ is mainly fixed by the resolution conditions, it is assumed to be the same for the two contributions ($\Gamma \approx 0.4$–0.8 meV). Together with the background, the agreement with the experiments, shown by the solid lines, is good. The values obtained for $E_\pm$ as a function of Q_a are shown in Fig. 4. We establish several new features. At both Q_b^{AF} (open symbols) and Q_b^{ZC} (solid symbols), the transverse dispersion consists of two distinct excitation branches which never cross. This justifies our previous statement, namely, that there are *two* distinct energy gaps, E_g^+ and E_g^-. In each branch, the periodicity is $2\pi Q_a$: this is twice that previously determined. The two dispersions have the same amplitude, $\delta J \approx 1$ meV but, remarkably, the upper and lower branches are out of phase, and there is phase inversion between branches at Q_b^{ZC} and Q_b^{AF}. For each excitation branch, the corresponding structure factors, $S_{b\pm}^{\mathrm{AF}}(Q_a)$ and $S_{b\pm}^{\mathrm{ZC}}(Q_a)$ are evaluated by integrating the fitted dynamical response functions over a wide energy range (from 0 up to $E \approx 300\Gamma$). We estimate systematic error for varying the upper cutoff alters the results by at most 5%. The resulting values (dots and squares) are reported in Figs. 5a and 5b. The sums $S_b^{\mathrm{AF}}(Q_a) = S_{b+}^{\mathrm{AF}}(Q_a) + S_{b-}^{\mathrm{AF}}(Q_a)$ and $S_b^{\mathrm{ZC}}(Q_a) = S_{b+}^{\mathrm{ZC}}(Q_a) + S_{b-}^{\mathrm{ZC}}(Q_a)$ are shown as the stars.

The interpretation of these results is developed in three steps. First, the charge order: each spin is associated with an electronic wave function on the two sites of a rung that depends on $n_\pm$. The structure factors for the in-line and zigzag models are $S_{Q_b}(Q_a,\omega) = \cos^2(\pi Q_a \rho) \times \tilde{S}(Q_a, Q_b, \omega) + \Delta_c^2 \sin^2(\pi Q_a \rho)\tilde{S}(Q_a + \frac{1}{2}, Q_b, \omega)$ and $S_{Q_b}(Q_a,\omega) = \cos^2(\pi Q_a \rho)\tilde{S}(Q_a, Q_b, \omega) + \Delta_c^2 \sin^2(\pi \times Q_a \rho)\tilde{S}(Q_a + \frac{1}{2}, Q_b + \frac{1}{2}, \omega)$, respectively, with $\omega = E/\hbar$ and where $\rho = l/a \approx 0.304$ (l, rung length and a, lattice parameter), and $\tilde{S}(Q_a, Q_b, \omega)$ is the structure factor for spins localized on the center of each rung [15]. From the ratios of intensities for different values of momentum, one can extract the charge transfer Δ_c independent of the form of $\tilde{S}$. In particular, we verify that the order cannot be in line but predictions agree with a zigzag order with $\Delta_c^2 \approx 0.35$, i.e., $\Delta_c \approx 0.6$. The agreement is particularly good for the sums $S_b^{\mathrm{AF}}(Q_a)$ and $S_b^{\mathrm{ZC}}(Q_a)$. For the absolute intensities, we need an explicit form for $\tilde{S}$ which we take from the strongly dimerized limit (SDL), in which the wave function is simply a product of singlets on the stronger bonds. For the in-line model, for example, the SDL would give zero intensity at Q_b^{ZC} in contradiction with the observation (the data in Fig. 5b). The in-line model can be ruled out. In Figs. 5a and 5b, the predictions provided by the zigzag model (solid lines) are compared with the experimental total structure factors $S_b^{\mathrm{AF}}(Q_a)$ and $S_b^{\mathrm{ZC}}(Q_a)$ (solid and open stars). In Fig. 5a, the agreement is obtained with no adjustable parameter except for an overall amplitude factor. Once this factor is determined, the results in Fig. 5b depend only on Δ_c^2. As can be seen, a good agreement is obtained for $\Delta_c^2 \approx 0.35$. The low-T phase of NaV_2O_5 is very well described by the zigzag model, with a rather large charge transfer.

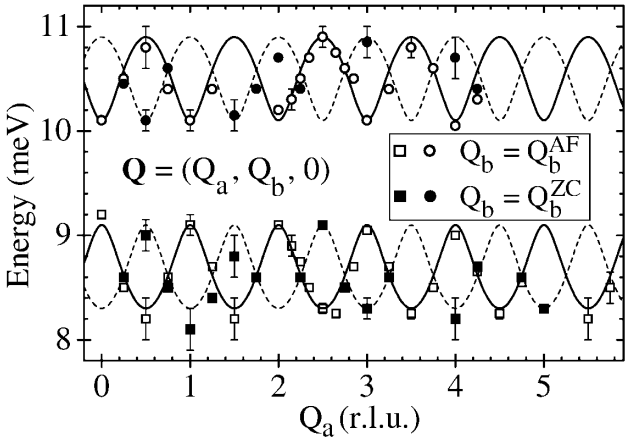

FIG. 4. Dispersion of the two excitation branches in the **a** direction at Q_b^{AF} and Q_b^{ZC}. The curves are theoretical predictions fitted to the data (see text).

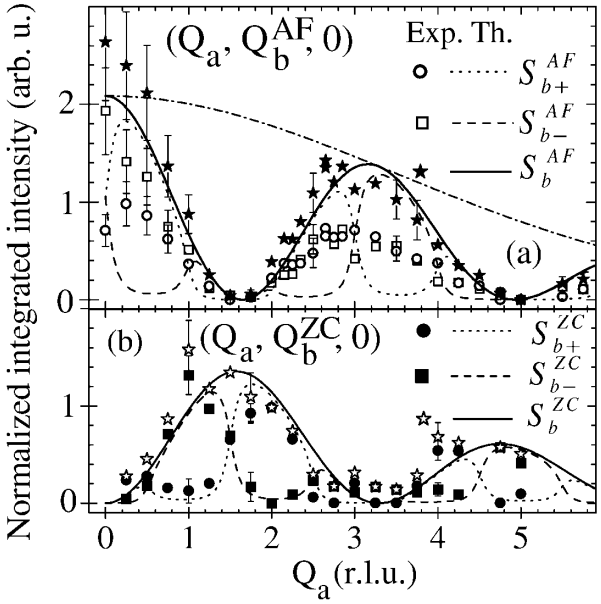

FIG. 5. Structure factors $S_{b\pm}^{\mathrm{AF}}(Q_a)$ and $S_{b\pm}^{\mathrm{ZC}}(Q_a)$ for the two magnetic branches in the **a** direction: (a) at Q_b^{AF}; (b) at Q_b^{ZC}. The solid and open stars represent the sums $S_b^{\mathrm{AF}}(Q_a)$ and $S_b^{\mathrm{ZC}}(Q_a)$. The data are corrected from the V^{4+} atomic form factor $f_{V^{4+}}$, being all normalized at $Q_b = 0.5$. The dot-dashed line gives the Q_a dependence of $f_{V^{4+}}$. The other curves are theoretical predictions compared to the experiments (see text).

Second, we consider the transverse dispersions. Later, we explain that the gap is induced by the CO. In fact, there are two distinct gaps because of the structural distortions (implying distinct couplings $J^A_{b1,2}$ and $J^B_{b1,2}$ as shown in Fig. 1b). Because of the CO, four different interchain exchange integrals must be considered, J'_1, J'_2, J'_3, and J'_4. The two branches (associated with the gaps E_g^+ and E_g^-) acquire a transverse dispersion, described at Q_b^{AF} and Q_b^{ZC} by $E^{\mathrm{AF}}_{b\pm} = (E_g^+ + E_g^-)/2 \pm \sqrt{(E_g^+ - E_g^-)^2/4 + \delta J^2 \sin^2(\pi Q_a)}$ and $E^{\mathrm{ZC}}_{b\pm} = (E_g^+ + E_g^-)/2 \pm \sqrt{(E_g^+ - E_g^-)^2/4 + \delta J^2 \cos^2(\pi Q_a)}$, respectively, with $\delta J = J'_1 - J'_2 + J'_3 - J'_4$ [15]. In Fig. 4, these predictions (solid and dashed lines) are compared to the data. Again, a very good agreement is obtained yielding the following evaluation $E_g^+ = 10.1 \pm 0.1$, $E_g^- = 9.1 \pm 0.1$ and $\delta J = 1.2 \pm 0.1$ meV. The dispersion gives directly the *alternation* in the interladder diagonal bonds δJ. If we assume it is dominated by the CO, we can also estimate the *average* from $\delta J \approx J_\perp \Delta_c^2$ [12] giving $J_\perp \approx 2.4$ meV.

The structure factors can be calculated for each branch. Within the SDL approach, one obtains the contributions $S^{\mathrm{AF}}_{b\pm}(Q_a)$ and $S^{\mathrm{ZC}}_{b\pm}(Q_a)$ [16] shown by the dotted and dashed lines in Fig. 5. In Fig. 5b, the agreement with the data is rather good. In particular, the extinction phenomenon observed for each branch is well reproduced. In Fig. 5a, while the sum $S_b^{\mathrm{AF}}(Q_a)$ is well described, we note a discrepancy between the SDL predictions and the *individual* structure factors $S^{\mathrm{AF}}_{b+}(Q_a)$ and $S^{\mathrm{AF}}_{b-}(Q_a)$. This difficulty could be explained as follows. As shown in Fig. 1b, two successive chains are not identical. A charge transfer giving different average valence on the chains will mix intensities at Q_b^{AF} without affecting the fluctuations at Q_b^{ZC} in qualitative agreement with the observation [17]. Experimental supports for such a charge transfer would be useful. Our proposition for the charge ordering, i.e., the zigzag model sketched in Fig. 1a, and our estimate $\Delta_c \approx 0.6$ are based on the *total* intensities.

Finally, we consider the origin of the gap. As discussed in the introduction, the lattice distortion alone, in isolated ladders, cannot explain the presence of two energy gaps and their size. To analyze the effects of the diagonal couplings $J_\perp$, we refer to Fig. 1b. Each ladder is seen to be a succession of two distinct clusters (shown by ovals in the figure). By exact diagonalization of each cluster, using the effective parameters of a t-J model [10] and adding a potential imposing a charge transfer, we evaluated J_{b1} and J_{b2} as a function of Δ_c and the bond alternation $d = |J_{b1} - J_{b2}|/(J_{b1} + J_{b2})$. For $\Delta_c \approx 0.6$, the couplings underestimate the experimental value by a factor of about 2, but as the parameters calculated on the high temperature structure [10] and as such cluster calculations are rather crude, the agreement is satisfactory. The value obtained for the bond alternation can be considered as reasonable: $d \approx 0.025-0.030$. Then, using the experimental value $J_b \approx 60$ meV, one finds an energy gap $E_g \approx 6-8$ meV. This is in fairly good agreement with the experimental value $E_g \approx 10$ meV. This simple analysis supports the view that, in NaV_2O_5, the gaps are primarily due to the CO [18]. The lattice distortion plays a secondary role, explaining why two distinct branches are observed experimentally, and their separation. In our picture, the magnetic anisotropies are unnecessary [7].

In conclusion, the CO in NaV_2O_5 is quantitatively determined by the present NIS measurements [19]. It explains also the energy gaps observed in the low-T phase of this compound.

[1] M. Isobe and Y. Ueda, J. Phys. Soc. Jpn. **65**, 1178 (1996).
[2] T. Chatterji *et al.,* Solid State Commun. **108**, 23 (1998).
[3] T. Yosihama *et al.,* J. Phys. Soc. Jpn. **67**, 744 (1998).
[4] S. G. Bompadre *et al.,* cond-mat/9911298.
[5] M. Mostovoy and D. Khomski, cond-mat/9806215; A. Damascelli *et al.,* Phys. Rev. Lett. **81**, 918 (1998); P. Thalmeier and P. Fulde, Europhys. Lett. **44**, 142 (1998); H. Seo and K. Fukuyama, J. Phys. Soc. Jpn. **67**, 2602 (1998); J. Riera *et al.,* Phys. Rev. B **59**, 2667 (1999); A. I. Smirnov *et al., ibid.* **59**, 14 546 (1999); H. Schwenk *et al., ibid.* **60**, 9194 (1999); M. Lohmann *et al.,* Phys. Rev. Lett. **85**, 1742 (2000).
[6] T. Ohama *et al.,* Phys. Rev. B **59**, 3299 (1999).
[7] P. Thalmeier and A. N. Yaresko, Eur. J. Phys. B **14**, 495 (2000).
[8] P. A. Carpy and J. Galy, Acta Crystallogr. Sect. B **31**, 1481 (1975).
[9] H. Smolinski *et al.,* Phys. Rev. Lett. **80**, 5164 (1998).
[10] N. Suaud and M. B. Lepetit, Phys. Rev. B **62**, 402 (2000).
[11] J. Lüdecke *et al.,* Phys. Rev. Lett. **82**, 3633 (1999).
[12] C. Gros and R. Valenti, Phys. Rev. Lett. **82**, 976 (1999).
[13] Taking into account an estimated magnetic contribution for this temperature.
[14] T. E. Mason *et al.,* Phys. Rev. Lett. **69**, 490 (1992).
[15] O. Cepas, Ph.D. thesis, Université J. Fourier Grenoble I, France, 2000.
[16] The corresponding expressions agree with the sum rules $S_b^{\mathrm{AF}}(Q_a)$ and $S_b^{\mathrm{ZC}}(Q_a)$ established above.
[17] In contrast, if we assume different values of Δ_c on two successive chains, the individual modes will mix at Q_b^{ZC} rather than at Q_b^{AF} unlike what is observed.
[18] In T. Ohama *et al.,* cond-mat/0003141, the CO proposed in model Z2 (Fig. 3) does not give rise to energy gaps; model Z3 provides a gap for only one out of two chains, and model Z1 is magnetically equivalent to ours (Fig. 1b).
[19] Other models assuming three different valence states (V^{4+}, $V^{4.5+}$, and V^{5+}) have been shown to be incompatible with our results: S. Trebst *et al.,* Phys. Rev. B **62**, R14 613 (2000); C. Gros *et al., ibid.* **62**, R14 617 (2000), and references therein.